Control of gating mode by a single amino acid residue in transmembrane segment IS3 of the N-type Ca^{2+} channel

Huijun Zhong*, Bin Li*, Todd Scheuer, and William A. Catterall†

Department of Pharmacology, Mailstop 357280, University of Washington, Seattle, WA 98195-7280

Contributed by William A. Catterall, December 28, 2000

N-type Ca^{2+} channels can be inhibited by neurotransmitter-induced release of G protein $\beta\gamma$ subunits. Two isoforms of $Ca_v2.2$ $\alpha1$ subunits of N-type calcium channels from rat brain ($Ca_v2.2a$ and $Ca_v2.2b$; initially termed rbB-I and rbB-II) have different functional properties. Unmodulated $Ca_v2.2b$ channels are in an easily activated "willing" (*W*) state with fast activation kinetics and no prepulse facilitation. Activating G proteins shifts $Ca_v2.2b$ channels to a difficult to activate "reluctant" (*R*) state with slow activation kinetics; they can be returned to the *W* state by strong depolarization resulting in prepulse facilitation. This contrasts with $Ca_v2.2a$ channels, which are tonically in the *R* state and exhibit strong prepulse facilitation. Activating or inhibiting G proteins has no effect. Thus, the *R* state of $Ca_v2.2a$ and its reversal by prepulse facilitation are intrinsic to the channel and independent of G protein modulation. Mutating G177 in segment IS3 of $Ca_v2.2b$ to E as in $Ca_v2.2a$ converts $Ca_v2.2b$ tonically to the *R* state, insensitive to further G protein modulation. The converse substitution in $Ca_v2.2a$, E177G, converts it to the *W* state and restores G protein modulation. We propose that negatively charged E177 in IS3 interacts with a positive charge in the IS4 voltage sensor when the channel is closed and produces the *R* state of $Ca_v2.2a$ by a voltage sensor-trapping mechanism. G protein $\beta\gamma$ subunits may produce reluctant channels by a similar molecular mechanism.

neuromodulation | G protein | voltage sensor | facilitation

Voltage-gated N-type Ca^{2+} currents play a central role in regulating the release of neurotransmitters (1–3), and N-type Ca^{2+} channels containing $Ca_v2.2$ $\alpha1$ subunits (4–6) are highly concentrated in nerve terminals (7, 8). N-type channels are inhibited by activation of G protein-coupled receptors (9), which regulate neurotransmitter release by means of a negative feedback loop (10, 11). G protein inhibition is mediated by $G\beta\gamma$ subunits (12, 13), which bind to multiple target sites in the intracellular loop connecting domains I and II ($L_{I\text{-}II}$) (14–17), the C terminus (18, 19), and the N terminus (20–23). Binding of G proteins is thought to cause a shift of gating mode from an easily activated "willing" (*W*) state to a "reluctant" (*R*) state (24). Strong depolarization shifts the channels back from the *R* state to the *W* state, producing prepulse facilitation (9, 25, 26).

Several different isoforms of $Ca_v2.2$ sharing >90% overall sequence identity have been cloned and functionally characterized (4, 5, 27–31). N-type Ca^{2+} channels cloned from rat brain have two isoforms, $Ca_v2.2a$ and $Ca_v2.2b$ originally designated rbB-I and rbB-II (4, 27, 29). In this study, we have examined the mechanism of G protein modulation and voltage-dependent facilitation of these two channel isoforms. Our results show that the $Ca_v2.2a$ channel has intrinsic prepulse facilitation that is independent of G proteins, as if this channel is tonically in the *R* state, whereas the $Ca_v2.2b$ channel shows G protein-dependent inhibition and prepulse facilitation consistent with the *W* state. This difference in channel gating and G protein modulation depends on a single amino acid difference in transmembrane segment IS3. The results lead to the conclusion that the reluctant state is intrinsic to the $Ca_v2.2a$ channel in the absence of bound G protein. A voltage sensor-trapping mechanism, in which an S4 voltage sensor is stabilized in its inward, not-activated position, is proposed to account for the effect of this single amino acid difference and for modulation by $G\beta\gamma$.

Experimental Procedures

Materials. A recombinant cDNA encoding $Ca_v2.2a$ from rat brain [originally called rbB-I (4)] was subcloned into pCDNA3 (Invitrogen). The cDNA encoding the $Ca_v2.2b$ isoform was identical to rbB-II (29), except for insertion of A at position 415 in $L_{I\text{-}II}$. It was subcloned into pMRC-CMV (Invitrogen). The $\beta1b$ subunit was in the vector pMT2XS (27), $\alpha2\delta$ in pZEM228 (32), and CD8 in EBO-pcD. Site-directed mutagenesis to construct $Ca_v2.2a$ (E177G) was accomplished by replacing the *Bis*wI–*Srf*I fragment of $Ca_v2.2a$ with its corresponding fragment from $Ca_v2.2b$. Likewise, the $Ca_v2.2b$ (G177E) mutation was generated by replacing the *Bis*wI–*Srf*I fragment with its $Ca_v2.2a$ counterpart.

Expression and Electrophysiology. TsA-201 cells were maintained in DMEM/Ham's F-12 (1:1) supplemented with 10% FBS (Life Technologies, Rockville, MD) at 37°C under 10% CO_2. Cells plated in 35-mm tissue culture dishes were grown to 60–80% confluence and transfected by the Ca^{2+} phosphate method with a total of 4 μg DNA including a 1:1 molar ratio of cDNAs encoding Ca^{2+} channel subunits and 0.3 μg of a CD8 expression plasmid for identification of transfected cells. The cells were subcultured at 24 h after the transfection. At least 48 h after transfection, positive transfected cells were visually identified by labeling with CD8-antibody-coated beads. Barium currents were recorded by the whole-cell patch clamp technique by using a List EPC-7 amplifier and filtered at 5 kHz with an eight-pole Bessel filter. Leak and capacitance currents were measured and subtracted by using the p/−4 method. The extracellular recording solution contained 120 mM Tris, 4 mM $MgCl_2$, and 10 mM $BaCl_2$ with pH adjusted to 7.3 by methanesulfonic acid. The internal pipette solution consisted of 120 mM aspartic acid, 5 mM $CaCl_2$, 2 mM $MgCl_2$, 10 mM Hepes, 10 mM EGTA, and 2 mM Mg-ATP with pH adjusted to 7.3 by CsOH. In some experiments, guanosine 5′-[γ-thio] triphosphate (GTPγS) was added to the internal solution at a concentration of 0.2 mM. Where indicated, guanosine 5′-*O*-(2-thiodi-phosphate) (GDPβS) was added to the internal solution to give a concentration of 2.0 mM. Somatostatin was dissolved in water to give a stock solution of 1 mM and added to the extracellular solution at a final concentration of 1 μM. *N*-Ethylmaleimide (NEM) were prepared in distilled water at 50

Abbreviation: *W*, willing; *R*, reluctant; GTPγS, guanosine 5′-[γ-thio] triphosphate; GDPβS, guanosine 5′-*O*-(2-thiodi-phosphate); NEM, *N*-ethylmaleimide.

*H.Z. and B.L. contributed equally to this work

†To whom reprint requests should be addressed. E-mail: wcatt@u.washington.edu.

The publication costs of this article were defrayed in part by page charge payment. This article must therefore be hereby marked "*advertisement*" in accordance with 18 U.S.C. §1734 solely to indicate this fact.

NEUROBIOLOGY

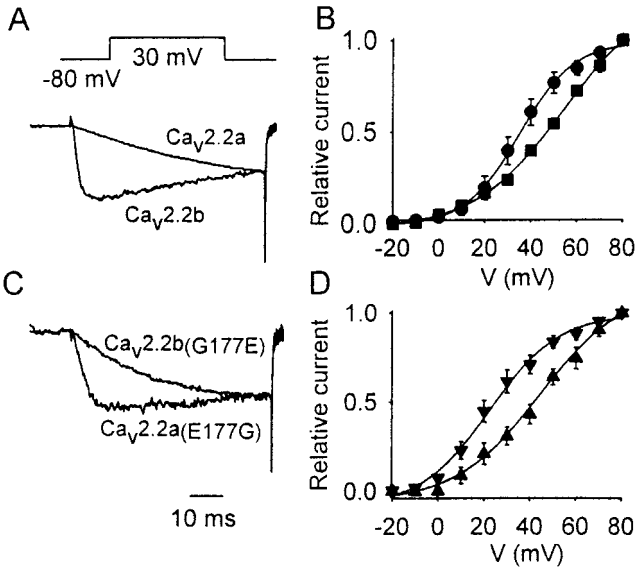

Fig. 1. Kinetics and voltage-dependence of activation of $Ca_v2.2a$, $Ca_v2.2b$, and mutant $Ca_v2.2$ channels. (*A*) Ionic currents of $Ca_v2.2a$ and $Ca_v2.2b$ channels. Example current traces were recorded during a 50-ms test pulse to +30 mV from the holding potential of −80 mV. (*Inset*) Voltage-clamp protocol. (*B*) Voltage dependence of activation of $Ca_v2.2a$ (■) and $Ca_v2.2b$ (●). Tail currents were recorded after test pulses to the indicated potentials from a holding potential of −80 mV, as in *A*, and normalized to the largest tail current in each series of test pulses. Mean ± SEM were plotted against test pulse potentials. (*C*) Ionic currents of $Ca_v2.2a(E177G)$ and $Ca_v2.2b(G177E)$. Example current traces were recorded during a 50-ms test pulse to +30 mV from the holding potential of −80 mV. (*D*) Voltage dependence of activation of the mutations $Ca_v2.2a$ (E177G) (▼) and $Ca_v2.2b(G177E)$ (▲). Tail currents were normalized to the largest tail current in each series of test pulses, and mean ± SEM, were plotted against test pulse potentials.

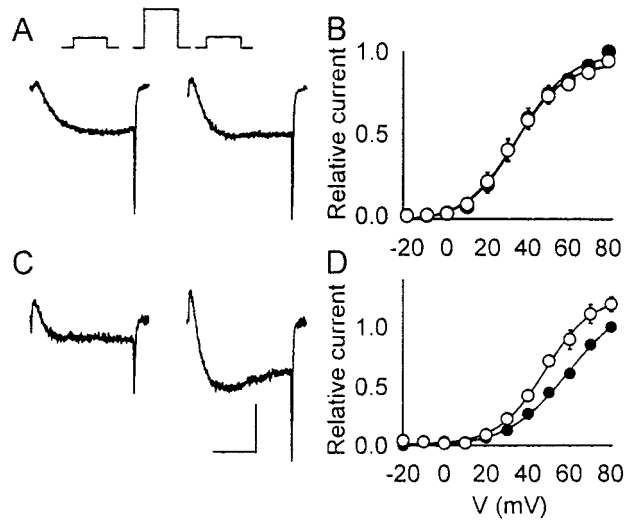

Fig. 2. Intrinsic and GTPγS-induced facilitation of $Ca_v2.2b$ channels. (*A*) Prepulse facilitation of the rate of activation without GTPγS. A 10-ms test pulse (test 1) to +30 mV was applied from the holding potential of −80 mV. After 3 s, a 10-ms conditional prepulse to 100 mV was applied, the cell was repolarized to −80 mV for 1 ms, and a second 10-ms test pulse (test 2) identical to the first test pulse was applied. (*Inset*) Voltage clamp protocol. (*B*) Prepulse facilitation of the voltage dependence of activation without GTPγS. Tail currents were recorded following test 1 (●) and test 2 (○) at the indicated membrane potentials as described in *A*. Mean ± SEM of tail currents are plotted vs. test potential. (*C*) Prepulse facilitation of the rate of activation with 0.2 mM GTPγS, measured as in *A*. (*D*) Prepulse facilitation of the voltage dependence of activation with 0.2 mM GTPγS, measured as in *B*. (Scale bars: 0.1 nA, 4 ms.)

mM and added to the extracellular solution to give a final concentration of 50 μM. All agents were purchased from Sigma unless otherwise mentioned. All averaged values represent mean ± SEM.

Results

Kinetics and Voltage-Dependence of Activation of Different $Ca_v2.2$ Channels. Ca^{2+} channels consisting of the $Ca_v2.2a$ or $Ca_v2.2b$ α_1 subunits, $\alpha_2\delta$ subunits, and β_{1b} subunits were expressed in the tsA-201 subclone of HEK293 cells as described in *Experimental Procedures*. These two Ca^{2+} channels have strikingly different functional properties (Fig. 1*A*). Ca^{2+} channels containing $Ca_v2.2b$ exhibit fast activation (τ_{act} = 1.42 ± 0.08 ms, n = 4) and inactivation (τ_{inact} = 128 ± 10.8 ms, n = 4). In contrast, $Ca_v2.2a$ activates and inactivates slowly (τ_{act} = 46.6 ± 5.3 ms, n = 6; τ_{inact} = 264 ± 28 ms, n = 6). In addition to this kinetic difference, the midpoint of the conductance–voltage curve of $Ca_v2.2a$ is more positive (V_a = 54.2 ± 2.2 mV, n = 16; Fig. 1*B*) and less steep in comparison to $Ca_v2.2b$ (V_a = 35.1 ± 5.4 mV, n = 18; Fig. 1*B*).

Effect of a Single Amino Acid Change in Transmembrane Segment IS3 on Activation of $Ca_v2.2$ Channels. There are at least four sites of alternative amino acid residues in $Ca_v2.2$: (*i*) a glycine (G) to glutamate (E) substitution at position 177 in segment S3 in domain I; (*ii*) an E to G substitution at position 387 in $L_{I\text{-}II}$; (*iii*) the absence of alanine (A) at position 415 in $L_{I\text{-}II}$; and (*iv*) the absence of SFMG in the S3–S4 linker in domain III. Previous experiments have shown that the amino acid sequence differences in $L_{I\text{-}II}$ and in segment IIIS3–S4 have small, but significant, effects on Ca^{2+} currents (30, 31). However, these sequence differences are not responsible for the major change in the rate and voltage dependence of activation illustrated in Fig. 1 *A* and *B*. To examine the functional properties of Ca^{2+} channels differing only at position 177, we analyzed $Ca_v2.2a(E177G)$ and $Ca_v2.2b(G177E)$ by whole-cell voltage clamp. $Ca_v2.2a(E177G)$ activated and inactivated rapidly like $Ca_v2.2b$ (Fig. 1*C*; τ_{act} = 1.39 ± 0.11 ms, n = 4; τ_{inact} = 128.2 ± 25.8 ms, n = 4). The converse mutation, $Ca_v2.2b(G177E)$, resulted in slow kinetics of activation, similar to $Ca_v2.2a$ (Fig. 1*C*; τ_{act} = 40.8 ± 8.7 ms, n = 4; τ_{inact} = 243 ± 45, n = 4). In addition, the voltage dependence of activation of these two mutants also was altered as expected if this single amino acid change is responsible for the functional differences between $Ca_v2.2a$ and $Ca_v2.2b$ (Fig. 1*D*). For $Ca_v2.2a(E177G)$, V_a was 23.6 ± 3.9 mV (n = 6), similar to $Ca_v2.2b$. Conversely, for $Ca_v2.2b(G177E)$, V_a was 44.3 ± 2.8 mV (n = 9), more than 10 mV positive to wild-type $Ca_v2.2b$ and similar to wild-type $Ca_v2.2a$. Thus, the amino acid residue at position 177 is responsible for nearly all of the difference in kinetics and voltage dependence of activation between $Ca_v2.2a$ and $Ca_v2.2b$.

G Protein Activation and Prepulse Facilitation of $Ca_v2.2$ Channel Isoforms. The slow activation kinetics and positive voltage dependence of activation of $Ca_v2.2a$ resemble N-type Ca^{2+} channels following G protein modulation. To examine G protein modulation of these Ca^{2+} channels, we induced prepulse facilitation without and with GTPγS in the recording pipette to activate endogenous G proteins (see *Inset* to Fig. 2*A*). Facilitation during the prepulse was assessed by comparing the tail current following Test Pulse 2 to the tail current following Test Pulse 1. In the absence of G protein modulation, $Ca_v2.2b$ channels activate rapidly at relatively negative membrane potentials (Fig. 2 *A* and *B*). A depolarizing prepulse has no effect on the rate or voltage dependence of activation (Fig. 2 *A* and *B*). Activation of G proteins with GTPγS slows activation of $Ca_v2.2b$

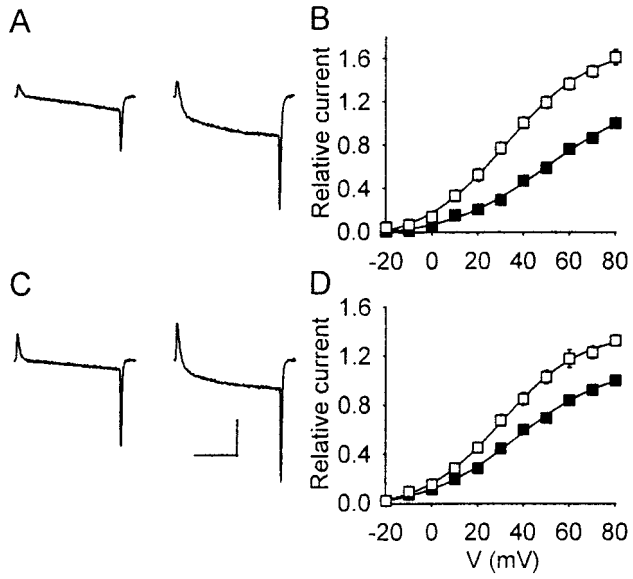

Fig. 3. Intrinsic and GTPγS-induced facilitation of $Ca_v2.2a$ channels. (*A*) Prepulse facilitation of the rate of activation without GTPγS. A 10-ms test pulse (test 1) to +30 mV was applied from the holding potential of −80 mV. After 3 s, a 10-ms conditioning prepulse to 100 mV was applied, the cell was repolarized to −80 mV for 1 ms, and a second 10-ms test pulse (test 2) identical to the first test pulse was applied. (*B*) Prepulse facilitation of the voltage dependence of activation without GTPγS. Tail currents were recorded following test 1 (■) and test 2 (□) at the indicated membrane potentials as described in *A*. Mean ± SEM of tail currents are plotted vs. test potential. (*C*) Prepulse facilitation of the rate of activation with 0.2 mM GTPγS in the intracellular solution, measured as in *A*. (*D*) Prepulse facilitation of the voltage dependence of activation with 0.2 mM GTPγS, measured as in *B*. (Scale bars: 0.2 nA, 4 ms.)

and shifts its voltage dependence of activation to more positive membrane potentials (Fig. 2 *C* and *D*). Depolarizing prepulses cause an obvious facilitation (Fig. 2 *C* and *D*), resulting from voltage-dependent reversal of G protein inhibition.

In contrast to these results with $Ca_v2.2b$, $Ca_v2.2a$ channels are slowly activated and have strong prepulse facilitation without G protein activation (Fig. 3 *A* and *B*). Activation of G proteins by GTPγS has no further effect on the kinetics or voltage dependence of activation or on prepulse facilitation (Fig. 3 *C* and *D*). These results indicate that the $Ca_v2.2a$ channel has intrinsic facilitation, independent of G protein modulation.

To test whether the prepulse facilitation of $Ca_v2.2a$ is truly independent of G protein action, we examined the effects of G protein inhibitors. Inhibition of G protein activity by including GDPβS (2 mM) in the pipette had no effect on prepulse facilitation of $Ca_v2.2a$ (33). The sulfhydryl reagent NEM is a more potent inhibitor of G protein action (34). Addition of 50 μM NEM to the extracellular solution blocked somatostatin-induced facilitation of $Ca_v2.2b$ in our transfected cells, confirming that it is an effective inhibitor of G protein modulation of these Ca^{2+} channels (data not shown). NEM also blocked facilitation of $Ca_v2.2b$ channels, which is observed in a small percentage of cells in the absence of GTPγS stimulation (Fig. 4*A*). This indicates that the rare cells having measurable facilitation of $Ca_v2.2b$ channels in the absence of GTPγS have constitutively active G proteins, which cause tonic inhibition of Ca^{2+} currents and allow prepulse facilitation (Fig. 4*A*). In most cells expressing $Ca_v2.2b$, no measurable facilitation is observed in the absence of GTPγS, and NEM has no effect on Ca^{2+} channel function (data not shown). In contrast to these results with $Ca_v2.2b$, NEM had no effect on facilitation of Ca^{2+} currents conducted by $Ca_v2.2a$ (Fig. 4*B*). These results support the conclusion that facilitation of $Ca_v2.2a$ is intrinsic to the Ca^{2+} channel and does not require G proteins. Evidently, the Ca^{2+} channel itself is capable of entering a slowly activated, reluctant state that is responsive to prepulse facilitation.

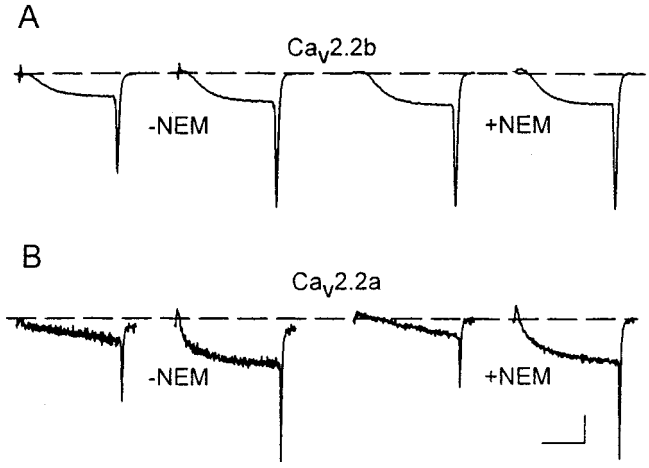

Fig. 4. Effect of NEM on prepulse facilitation of $Ca_v2.2a$ and $Ca_v2.2b$ channels. (*A*) Prepulse facilitation of $Ca_v2.2b$ channels, recorded as in Fig. 2*A* in the presence and absence of 50 μM NEM. (*B*) Prepulse facilitation of $Ca_v2.2b$ channels, measured as in Fig. 2*A* in the presence and absence of 50 μM NEM. (Scale bars: *A*, 1.5 nA, 4 ms; *B*, 0.2 nA, 4 ms.)

Effect of the Amino Acid at Position 177 on G Protein Modulation. To determine whether the amino acid at position 177 affects G protein modulation, we performed prepulse facilitation experiments with $Ca_v2.2a$(E177G). These mutant channels have fast activation without a depolarizing prepulse, and it is not further accelerated after a depolarizing prepulse (Fig. 5*A*). Similarly, the voltage dependence of activation of $Ca_v2.2a$(E177G) is also unaffected by a depolarizing prepulse (Fig. 5*B*). In addition, this

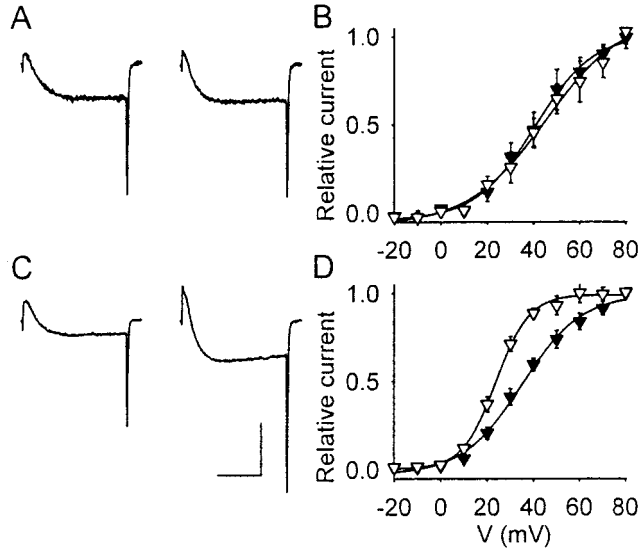

Fig. 5. Intrinsic and GTPγS-induced facilitation of $Ca_v2.2a$(E177G) channels. (*A*) Prepulse facilitation of the rate of activation without GTPγS, measured as described in Fig. 2*A*. (*B*) Prepulse facilitation of the voltage dependence of activation without GTPγS. Tail currents were recorded following test 1 (▼) and test 2 (▽) at the indicated membrane potentials as described in *A*. Mean ± SEM of tail currents are plotted vs. test potential. (*C*) Prepulse facilitation of the rate of activation with 0.2 mM GTPγS in the intracellular solution, measured as in *A*. (*D*) Prepulse facilitation of the voltage dependence of activation with 0.2 mM GTPγS, measured as in *B*. (Scale bars: *A*, 0.2 nA, 4 ms; *B*, 2.6 nA, 4 ms.)

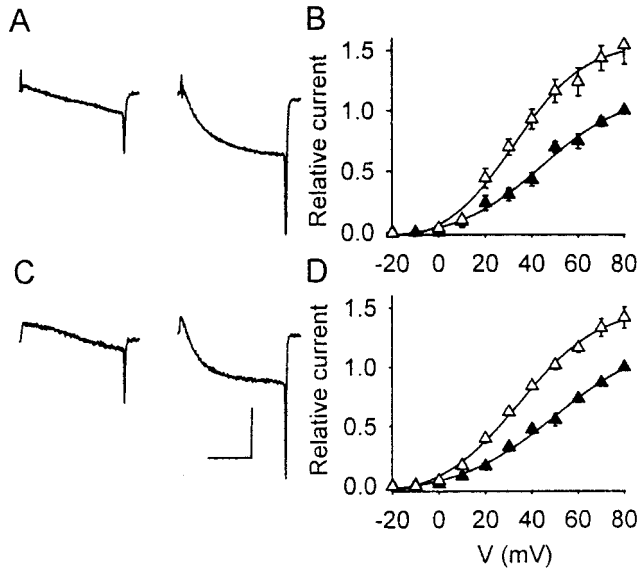

Fig. 6. Intrinsic and GTPγS-induced facilitation of $Ca_v2.2b$(G177E) channels. (*A*) Prepulse facilitation of the rate of activation without GTPγS, measured as in Fig. 2*A*. (*B*) Prepulse facilitation of the voltage dependence of activation without GTPγS. Tail currents were recorded following test 1 (▲) and test 2 (△) at the indicated membrane potentials as described in *A*. Mean ± SEM of tail currents are plotted vs. test potential. (*C*) Prepulse facilitation of the rate of activation with 0.2 mM GTPγS in the intracellular solution, measured as in *A*. (*D*) Prepulse facilitation of the voltage dependence of activation with 0.2 mM GTPγS, measured as in *B*. (Scale bars: *A*, 0.2 nA, 4 ms; *B*, 0.16 nA, 4 ms.)

mutant channel is subject to G protein modulation, as determined by prepulse facilitation (Fig. 5 *C* and *D*). In the presence of GTPγS, facilitation is induced, and the voltage dependence of activation is shifted to more negative values by a depolarizing prepulse (Fig. 5*D*). On the other hand, $Ca_v2.2b$(G177E) has slow activation kinetics and strong prepulse facilitation in the absence of GTPγS, like $Ca_v2.2a$ (Fig. 6 *A* and *B*). This mutant is insensitive to further G protein modulation (Fig. 6 *C* and *D*). These results support the conclusion that the amino acid residue at position 177 in transmembrane segment IS3 determines the rate and voltage dependence of activation and the response to G proteins of the $Ca_v2.2$ channels.

Discussion

Regulation of $Ca_v2.2$ Channel Gating Mode by G Proteins. The mechanism of modulation of N-type Ca^{2+} channels by G protein-coupled receptors has been proposed to be a shift from a "willing" gating mode, in which Ca^{2+} channels activate rapidly upon depolarization, to a "reluctant" gating mode, in which activation is slow and requires a more positive depolarization (24). In the accompanying article (33), we show that an allosteric model based on this idea successfully accounts for regulation by Gβγ, prepulse facilitation, protein kinase C, and $Ca_v\beta$ subunits, which are proposed to alter the equilibrium constant for the transition between *R* and *W* states. Allosteric regulation of Ca^{2+} channel gating mode by these disparate agents implies that the *R* and *W* states are intrinsic to the Ca^{2+} channel α1 subunit, and the equilibrium constant for the transition between them is shifted by these different effectors. Consistent with that idea, we show in this report that $Ca_v2.2$ channels can be maintained in the *R* state in the absence of G protein activation by a single change in amino acid sequence in their α1 subunit.

$Ca_v2.2a$ Channels Are in a Reluctant Gating Mode Without Bound Gβγ. We have shown that $Ca_v2.2$ channels containing $Ca_v2.2a$ and $Ca_v2.2b$ α_1 subunits have intrinsic functional properties resembling the reluctant and willing gating modes, respectively. $Ca_v2.2b$ activated more rapidly and at much more negative membrane potentials than $Ca_v2.2a$. Activation of G proteins with GTPγS slowed activation of $Ca_v2.2b$ and shifted the voltage dependence of activation to more positive membrane potentials, but had no effect on these properties of $Ca_v2.2a$. Thus, G protein modulation is occluded in $Ca_v2.2a$ channels, as if they are in an *R* state under basal conditions. Prepulse-dependent facilitation is observed for $Ca_v2.2a$ in the absence of GTPγS, consistent with these channels being in a reluctant gating mode without G protein activation. In contrast, $Ca_v2.2b$ requires G protein activation and the resulting slowing of activation and positive shift of its voltage dependence for prepulse facilitation. The functional properties and prepulse facilitation of $Ca_v2.2a$ are not affected by inhibition of endogenous G proteins with GDPβS or NEM. The results with NEM are especially persuasive because this reagent is a noncompetitive inhibitor of G protein signaling whose action is not opposed by GTP or effector binding (34). Altogether, these results indicate that the $Ca_v2.2a$ isoform of $Ca_v2.2$ channels is constitutively in a reluctant gating mode without G protein binding and can be shifted to the willing gating mode by depolarizing prepulses.

The Amino Acid At Position 177 in IS3 Determines Gating Mode. Although there are at least four sites of molecular differences between $Ca_v2.2a$ and $Ca_v2.2b$, our results show that the differences in the kinetics and voltage dependence of activation and in the response to G proteins between these Ca^{2+} channels are determined primarily by the identity of the amino acid at position 177. When a glycine is present at this position, the channels are in a willing gating mode and are subject to G protein inhibition and subsequent prepulse facilitation. When a glutamate is present at this position, the channels are in a reluctant gating mode, strong prepulse facilitation is observed without G protein activation, and changes in the concentration of free Gβγ have little effect on channel function. Thus, the identity of this single amino residue determines the basal gating mode of $Ca_v2.2$ channels.

Although the gating and regulatory properties of $Ca_v2.2a$ closely resemble those of reluctant $Ca_v2.2b$ channels generated by activation of G proteins, detailed analysis revealed that activation is slower but is shifted less strongly toward positive potentials for $Ca_v2.2a$. Thus, the $Ca_v2.2a$ channel in its basal state is not quantitatively identical to $Ca_v2.2b$ after G protein regulation, even though it shares the main functional features of a reluctant gating mode. Similarly, the kinetics and voltage dependence of the willing gating mode of $Ca_v2.2a$(E177G) are not quantitatively identical to $Ca_v2.2b$. One of the other sites of known amino acid sequence difference among these isoforms (29, 31) may be responsible for these subtle differences in kinetics of gating.

There are at least two possible mechanisms for the tonically reluctant gating mode of $Ca_v2.2a$. Either this channel is tonically in an *R* state in the absence of G protein binding, or it has exceptionally high affinity for G proteins and can be modulated by the low level of Gβγ present in unstimulated cells. Our data favor the first conclusion because the G protein inhibitors GDPβS and NEM did not shift these channels to the *W* state. Evidently, the presence of a glutamate at position 177 in transmembrane segment IS3 is sufficient to shift $Ca_v2.2$ channels to a reluctant gating mode without binding of Gβγ subunits.

A Voltage Sensor-Trapping Mechanism for G Protein Modulation of $Ca_v2.2$ Channels. Activation of voltage-gated sodium channels is initiated by the outward movement of positive gating charges in the S4 segments in each domain under the influence of the transmembrane electric field (35–39). Shift of N-type Ca^{2+} channels to the reluctant gating mode by G protein modulation slows the gating current caused by outward movement of the S4 voltage sensors preceding channel activation (40, 41), as if the outward movement of one or more S4 segments is slowed by Gβγ binding. Peptide

neurotoxins alter sodium channel gating by binding to the S3–S4 loop at the extracellular end of the voltage-sensing S4 segments and altering their transmembrane movement by voltage-sensor trapping (42, 43). In the case of α-scorpion toxins, the S4 segment in domain IV of sodium channels is trapped in an inward position, but prolonged, strong depolarization causes dissociation of the bound toxin (44, 45), perhaps because of the voltage-driven outward movement of the IVS4 segment. G$\beta\gamma$ subunits may act in an analogous manner by binding to target sites on the intracellular surface of $Ca_v2.2$ channels and holding an S4 segment in its inward, not-activated position by protein–protein interactions. This molecular interaction would shift the equilibrium toward the *R* state by decreasing the equilibrium constant K_{WR} in the allosteric model of G$\beta\gamma$ action described in the accompanying paper (33). Strong depolarization may push the S4 segment outward despite the bound G protein and thereby relieve G protein inhibition and favor channel activation.

The change of G177 to E in segment IS3 may also trap the S4 segment in an inward, not-activated position by electrostatic interactions. The positive charges in the S4 voltage sensors are thought to be stabilized in their membrane environment by ion pairing with negative charges in the S2 and S3 transmembrane segments (36). In support of this idea, a charge reversal mutation of E293 in S2 or D316 in S3 of Shaker potassium channels dramatically affects voltage-dependent gating (46–49). We propose that the negative charge at E177 forms a local electrostatic interaction with one of the positively charged residues of the IS4 segment. When this ion pair is formed, moving the IS4 segment outward would require more energy, and activation gating would be slowed and shifted to more positive potentials.

Although the Ca^{2+} channel has four voltage sensors, we find that a single mutation in transmembrane segment IS3 results in striking changes in kinetics and voltage dependence of activation. G177 speeds up activation of the channel, whereas E177 slows activation. These results indicate that the IS4 is the rate-limiting voltage sensor in the $Ca_v2.2a$ channel. The IS3 segment is a primary determinant of the rate of activation of Ca_v1 channels (50), consistent with the hypothesis that the change of G177 to E in IS3 of $Ca_v2.2$ may act through interaction with IS4 gating charges to oppose channel activation.

The voltage sensor trapping mechanism of action of G proteins on $Ca_v2.2$ channels implies that bound G protein $\beta\gamma$ subunits interact with the intracellular end of an S4 segment and hold it in an inward position. This interaction could be direct or mediated indirectly through one of the known G protein interaction sites on the $Ca_v2.2$ channel. The presence of G protein interaction sites (14–17), sites of protein kinase C modulation (17), and a site of $Ca_v\beta$ subunit binding (51) in $L_{I\text{-}II}$ points to the S4 segments in domains I and II as the most likely targets. Identification of a molecular interaction between G protein $\beta\gamma$ subunits and the intracellular end of an S4 segment would provide direct biochemical evidence for the voltage sensor-trapping mechanism of G protein action proposed here on the basis of functional studies.

We thank Dr. Charles Chavkin and Dr. Kenneth Mackie for comments on a draft of the manuscript. This work was supported by Research Grant N522625 from the National Institutes of Health to W.A.C. and a postdoctoral fellowship from the Medical Research Council of Canada to H.Z.

1. Hirning, L. D., Fox, A. P., McCleskey, E. W., Olivera, B. M., Thayer, S. A., Miller, R. J. & Tsien, R. W. (1988) *Science* **239,** 57–61.
2. Turner, T. J., Adams, M. E. & Dunlap, K. (1993) *Proc. Natl. Acad. Sci. USA* **90,** 9518–9522.
3. Dunlap, K., Luebke, J. I. & Turner, T. J. (1995) *Trends Neurosci.* **18,** 89–98.
4. Dubel, S. J., Starr, T. V. B., Hell, J., Ahlijanian, M. K., Enyeart, J. J., Catterall, W. A. & Snutch, T. P. (1992) *Proc. Natl. Acad. Sci. USA* **89,** 5058–5062.
5. Williams, M. E., Brust, P. F., Feldman, D. H., Patthi, S., Simerson, S., Maroufi, A., McCue, A. F., Velicelebi, G., Ellis, S. B. & Harpold, M. M. (1992) *Science* **257,** 389–395.
6. Ertel, E., Campbell, K. P., Harpold, M. M., Hofmann, F., Mori, Y., Perez-Reyes, E., Schwartz, A., Snutch, T., Tanabe, T., Birnbaumer, L., *et al.* (2000) *Neuron* **25,** 533–535.
7. Westenbroek, R. E., Hell, J. W., Warner, C., Dubel, S. J., Snutch, T. P. & Catterall, W. A. (1992) *Neuron* **9,** 1099–1115.
8. Westenbroek, R. E., Sakurai, T., Elliott, E. M., Hell, J. W., Starr, T. V. B., Snutch, T. P. & Catterall, W. A. (1995) *J. Neurosci.* **15,** 6403–6418.
9. Hille, B. (1994) *Trends Neurosci.* **17,** 531–536.
10. Lipscombe, D., Kongsamut, S. & Tsien., R. W. (1989) *Nature (London)* **340,** 639–642.
11. Brody, D. & Yue, D. (2000) *J. Neurosci.* **20,** 889–898.
12. Ikeda, S. R. (1996) *Nature (London)* **380,** 255–258.
13. Herlitze, S., Garcia, D. E., Mackie, K., Hille, B., Scheuer, T. & Catterall, W. A. (1996) *Nature (London)* **380,** 258–262.
14. Herlitze, S., Hockerman, G. H., Scheuer, T. & Catterall, W. A. (1997) *Proc. Natl. Acad. Sci. USA* **94,** 1512–1516.
15. De Waard, M., Liu, H. Y., Walker, D., Scott, V. E. S., Gurnett, C. A. & Campbell, K. P. (1997) *Nature (London)* **385,** 446–450.
16. Page, K. M., Stephens, G. J., Berrow, N. S. & Dolphin, A. C. (1997) *J. Neurosci.* **17,** 1330–1338.
17. Zamponi, G. W., Bourinet, E., Nelson, D., Nargeot, J. & Snutch, T. P. (1997) *Nature (London)* **385,** 442–446.
18. Furukawa, T., Nukada, T., Mori, Y., Wakamori, M., Fujita, Y., Ishida, H., Fukuda, K., Kato, S. & Yoshii, M. (1998) *J. Biol. Chem.* **273,** 17585–9498.
19. Qin, N., Platano, D., Olcese, R., Stefani, E. & Birnbaumer, L. (1997) *Proc. Natl. Acad. Sci. USA* **94,** 8866–8871.
20. Page, K. M., Cantí, C., Stephens, G. J., Berrow, N. S. & Dolphin, A. C. (1998) *J. Neurosci.* **18,** 4815–4824.
21. Canti, C., Page., K. M., Stephens, G. J. & Dolphin, A. C. (1999) *J. Neurosci.* **19,** 6855–6864.
22. Simen, A. A. & Miller, R. J. (1998) *J. Neurosci.* **18,** 3689–3698.
23. Simen, A. A. & Miller, R. J. (2000) *Mol. Pharmacol.* **57,** 1064–1074.
24. Bean, B. P. (1989) *Nature (London)* **340,** 153–156.
25. Marchetti, C., Carbone, E. & Lux, H. D. (1986) *Pflugers Arch.* **406,** 104–111.
26. Tsunoo, A., Yoshii, M. & Narahashi, T. (1986) *Proc. Natl. Acad. Sci. USA* **83,** 9832–9836.
27. Stea, A., Dubel, S. J., Pragnell, M., Leonard, J. P., Campbell, K. P. & Snutch, T. P. (1993) *Neuropharmacology* **32,** 1103–1116.
28. Coppola, T., Waldmann, R., Borsotto, M., Heurteaux, C., Romey, G., Mattéi, M.-G. & Lazdunski, M. (1994) *FEBS Lett.* **338,** 1–5.
29. Stea, A., Soong, T. W. & Snutch, T. P. (1995) *Neuron* **15,** 929–940.
30. Lin, Z. X., Haus, S., Edgerton, J. & Lipscombe, D. (1997) *Neuron* **18,** 153–166.
31. Lin, Z., Lin, Y., Schorge, S., Pan, J. Q., Beierlein, M. & Lipscombe, D. (1999) *J. Neurosci.* **19,** 5322–5331.
32. Ellis, S. B., Williams, M. E., Ways, N. R., Brenner, R., Sharp, A. H., Leung, A. T., Campbell, K. P., McKenna, E., Koch, W. J., Hui, A., *et al.* (1988) *Science* **241,** 1661–1664.
33. Herlitze, S., Zhong, H., Scheuer, T. & Catterall, W. A. (2001) *Proc. Natl. Acad. Sci. USA* **98,** 4699–4704.
34. Shapiro, M. S., Wollmuth, L. P. & Hille, B. (1994) *J. Neurosci.* **14,** 7109–7116.
35. Guy, H. R. & Seetharamulu, P. (1986) *Proc. Natl. Acad. Sci. USA* **83,** 508–512.
36. Catterall, W. A. (1986) *Trends Neurosci.* **9,** 7–10.
37. Stuhmer, W., Conti, F., Suzuki, H., Wang, X., Noda, M., Yahadi, N., Kubo, H. & Numa, S. (1989) *Nature (London)* **339,** 597–603.
38. Yang, N. B., George, A. L., Jr., & Horn, R. (1996) *Neuron* **16,** 113–122.
39. Catterall, W. A. (2000) *Neuron* **26,** 13–25.
40. Patil, P. G., De. Leon, M., Reed, R. R., Dubel, S., Snutch, T. P. & Yue, D. T. (1996) *Biophys. J.* **71,** 2509–2521.
41. Jones, L. P., Patil, P. G., Snutch, T. P. & Yue, D. T. (1997) *J. Physiol. (London)* **498,** 601–610.
42. Rogers, J. C., Qu, Y., Tanada, T. N., Scheuer, T. & Catterall, W. A. (1996) *J. Biol. Chem.* **271,** 15950–15962.
43. Cestèle, S., Qu, Y., Rogers, J. C., Rochat, H., Scheuer, T. & Catterall, W. A. (1998) *Neuron* **21,** 919–931.
44. Catterall, W. A. (1979) *J. Gen. Physiol.* **74,** 375–391.
45. Catterall, W. A. (1977) *J. Biol. Chem.* **252,** 8660–8668.
46. Papazian, D. M., Shao, X. M., Seoh, S.-A., Mock, A. F., Huang, Y. & Wainstock, D. H. (1995) *Neuron* **14,** 1293–1301.
47. Tiwari-Woodruff, S. K., Lin, M. A., Schulteis, C. T. & Papazian, D. M. (2000) *J. Gen. Physiol.* **115,** 123–138.
48. Seoh, S. A., Sigg, D., Papazian, D. M. & Bezanilla, F. (1996) *Neuron* **16,** 1159–1167.
49. Tiwari-Woodruff, S. K., Schulteis, C. T., Mock, A. F. & Papazian, D. M. (1997) *Biophys. J.* **72,** 1489–1500.
50. Nakai, J., Adams, B. A., Imoto, K. & Beam, K. G. (1994) *Proc. Natl. Acad. Sci. USA* **91,** 1014–1018.
51. Pragnell, M., De Waard, M., Mori, Y., Tanabe, T., Snutch, T. P. & Campbell, K. P. (1994) *Nature (London)* **368,** 67–70.